Water infiltration to soil column

Magdy M. Abo Elela

Department of Hydraulics and Irrigation, Faculty of Engineering, Alexandria University, Alexandria, Egypt

H. Zaradny

Institute of Hydroengineering, Polish Academy of Sciences, Gdansk, Poland

This paper presents a numerical method to solve the double phase flow, water and air. Among the numerical methods, the finite difference method has been chosen. The build up model (solved by the computer program CONDUCT written in FORTRAN) allows for a wide range of water infiltration problems into soil profiles. Also series of experimental tests were made on the column of soil (1-dimensional problem). They have been performed to better understand the mechanism of water and pore air movement as well as soil structure changes during the infiltration process.

يشتمل هذا البحث على نموذج رياضي لتمثيل حركة تدفق المياه والهواء داخل عمود أسطواني رأسي من التربة أثناء الأمطار الغزيـرة. كذلك يشتمل على عدد من التجارب المعملية التي أجريت على عمود أسطوانة رأسي من التربة لدراسة الظواهر الناشئة عـن تسـرب المياه الكثيفة داخل التربة. هذا وأجرى هذا البحث لدراسة ومعرفة ميكانيكية حركة المياه والهواء كذلك التغيرات الإنشائية للتربة وذلـك خلال عملية تسرب المياه خلالها.

Keywords: Infiltration, Pore air pressure, Double phase flow, Single-phase flow, Soil saturation.

1. Introduction

As was shown by the experimental results of Wilson and Luthin [1], Le van Phuc and Morel-Seytoux [2], Morel Seytoux [3], and others, the effect of air movement on the wetting front during water infiltration of soil is always very important. This is true even in the case of an unrestricted pore air contact with the atmosphere through the soil column.

In the case of a closed column, due to the wetting front displacement, the pressure of the soil air which resists water movement increases. This leads to a water flow in increasingly lesser pores (capillary effect). Wilson and Luthin [1] showed that the air is also present behind the wetting in increasing amounts as the pressure increases. The air is probably in continuous fingers protruding back from the front. As the front advances some of these fingers are isolated and the air remains in them in confinement. The fingers and confined air increase the tortuosity of the flow paths of the conducting channels and thus reduce the influx rate. This certainly will result in momentary balanced state (equilibrium) and its suddenly break. In this situation the air pressure could rise suddenly which may lead to its escape to the atmosphere, through the top part of the column.

This phenomenon is similar to the "stalking action" observed in capillary flow experiments. After air escape the infiltration velocity will generally violently increase, and later systematically reduce.

This type of result could be found among others in the work of McWhorter [4]. He conducted experiments on the infiltration of oil to sandstone of varying column length (185, 233, 393, and 990 cm) with closed and with open bottom. Results clearly show that the length of the column affects the infiltration curve shapes and the time of pore air escape through the column to the atmosphere. No structural changes in the column were noted. The result will be different in case of a normal soil structure. For such soil, after air escape, one can distinguish two layers: deeper undisturbed capped with more coarse, of higher permeability thinner layer (Morel-Seytoux [3]). More of this shall be mentioned with experimental results in this study. As a result even at infiltration intensity $q < K_{sat}$, the water content at soil surface could approach a value equal to θ_{sat} where θ_{sat} is the water content at full saturation. This will favor restriction on pore air contact with the atmosphere and thus lead to the increase in pore air pressure ($p_a > p_{atm}$).

2. Mathematical model for simultaneous water and air flow in soil

In case of double phase flow, i.e. liquid phase is water (quantity with index w) and gaseous phase is air (quantity with index a) a continuity equation for one dimensional flow (vertical column with z axis directed downwards) could be written as follows (Le van Phuc & H. J. Morel-Seytoux [2]:

$$\frac{\partial q_w}{\partial z} = -\varepsilon \frac{\partial S_w}{\partial t}, \tag{1}$$

$$\frac{\partial(\rho_a q_a)}{\partial z} = -\varepsilon \frac{\partial(\rho_a S_a)}{\partial t}, \tag{2}$$

where:

- q is the flow rate in the Darcy sense, [cm/s],
- S is the degree of saturation,($S_w+S_a=1$),
- ρ is the density or specific mass, [g/cm³],
- ε is the porosity,
- t is the time, [s],
- z is the elevation below reference datum, [cm].

The above is true for the assumption that during the period of recorded pressure changes the water density $\rho_w \approx$ constant that is equal in concept with the assumption that water is incompressible and therefore its specific mass (density) does not appear in Eq (1).

Flow rate according to Darcy can be represented as follows, (Le van Phuc & H. J. Morel-Seytoux [2]):

$$q_w = -k\frac{k_w^r}{\mu_w}\left(\frac{\partial p_w}{\partial z} - \rho_w g\right), \tag{3}$$

$$q_a = -k\frac{k_a^r}{\mu_a}\left(\frac{\partial p_a}{\partial z} - \rho_a g\right), \tag{4}$$

where:

k is the intrinsic permeability, [cm²],

k_a^r, k_w^r are the air and water relative permeability depending on degree of saturation, range of the value is (0, 1), respectively, [dimensionless],

μ_a, μ_w are the air and water dynamic viscosity, respectively, [g/cm.s],

p_a, p_w are the air and water pressure in the soil, respectively, [dynes/cm²],

g is the gravity acceleration, [cm/s²].

Assuming that capillary pressure $p_c=p_a-p_w$ is a known function of the soil saturation S_w and using the perfect gas law of an isothermal process, i.e. taking $p_a=\rho RT$ (among others, Duckworth [5]) and also utilising that $S_w+S_a=1$, one can obtain the motion equation as follows:

$$\frac{\partial S_w}{\partial t} = -\frac{1}{\varepsilon}\frac{\partial}{\partial z}\left[-k\frac{k_w^r}{\mu_w}\left\{\frac{\partial p_a}{\partial z} - \frac{\partial p_c}{\partial z} - \rho_w g\right\}\right], \tag{5}$$

$$\frac{\partial p_a}{\partial t} = -\frac{RT}{\varepsilon(1-S_w)}\left[\frac{\partial(\rho_a q_a)}{\partial z} + \rho_a\frac{\partial q_w}{\partial z}\right], \tag{6}$$

where:

- R is the perfect gas constant, for air R = 287 J/(kg·K),
- T is the air temperature in Kelvin ($T = 273.15 + T^*$, T^* is the temperature in °C).

Considering the earlier relationships and $p_a = \rho_a R T$, Eq. (6) can be further presented in the form:

$$\frac{\partial p_a}{\partial t} = -\frac{1}{\varepsilon(1-S_w)}\left[\frac{\partial(p_a q_a)}{\partial z} + p_a\frac{\partial q_w}{\partial z}\right]. \tag{7}$$

Relative permeability k_w^r and the relationship $P_c = f(S_w)$ could be defined according to Mualem [6] and van Genuchten [7]. For k_w^r, the following relation is obtained:

$$k_w^r = \frac{\left[1 - \frac{|\alpha h|^{n-1}}{(1+|\alpha h|^n)^m}\right]^2}{\left[1+|\alpha h|^n\right]^{\frac{m}{2}}}, \quad (8)$$

where:
m = 1 – 1/n (according to Mualem, [6]), [dimensionless],
α, n are the coefficients interrelated through S_w = f (h), [dimensionless],
h is the soil water pressure for $S_w < 1$ [cm].
Water saturation can be calculated from the formula:

$$S_w = \frac{1}{\left(1+|\alpha h|^n\right)^m} - S_{ra}, \quad (9)$$

where:
S_{ra} is the residual soil air saturation.

Put $S_w^* = S_w + S_{ra}$, the value of water pressure head in the soil can be obtained from the expression:

$$h = \frac{\left\{\left(S_w^*\right)^{-\frac{1}{m}} - 1\right\}^{\frac{1}{n}}}{\alpha}. \quad (10)$$

The value of capillary pressure, for $h \le 0$, can be obtained from the expression:

P_c = - 981.h (dynes/cm²).

And from the definition, for h > 0, the capillary pressure equals zero.

In the case of air, the value of k_a^r is determined according to Brooks & Corey [8]:

$$k_a^r = (1 - S_w)^2 \left\{1 - \frac{k_w^r}{\left(S_w^*\right)^2}\right\}. \quad (11)$$

Soil water saturation changes within the range:

$$S_{rw} \le S_w \le 1 - S_{ra},$$

where:

$$S_w = \frac{\theta}{\varepsilon},$$

S_{rw} is the residual soil water saturation.

Soil air saturation changes within the following range:

$$S_{ra} \le S_a \le 1 - S_{rw}.$$

The values of the pressures p_c, p_a and p_w must be expressed in dynes/cm² (for T*= 20 °C, $p_a = p_{atm}$= 102928 dynes/cm² and air density $\rho_a = p_a/(R.T)$=1.204.10⁻³ g/cm³
Where:

$$R = 287\ N \cdot m/(kg \cdot K) = 287 \times 10^4\ cm^2/(s^2 \cdot K))$$

For T* = 20 °C, the water density ρ_w is 0.998203 g/cm³, water viscosity μ_w is 1.002×10^{-2}g/(cm·s) and air viscosity μ_a is equal to 1.81×10^{-4}g/(cm.s). The hydraulic conductivity K_s of tested soil used in the experiments is K_s = 0.016 cm/s, and the corresponding intrinsic permeability value k = $K_s . \mu_w / (\rho_w . g) = 1.637 \times 10^{-7}\ cm^2 \approx 16{\cdot}6$ darcy (1 darcy = 0.98697 × 10^{-8} cm², Zaradny [9]).

The double phase flow problem (water and air) can be solved numerically. Among the numerical methods the finite difference method has been chosen. The flow region is divided into N space steps, Δz $(\Delta z = L/N)$, and the time under consideration t_{max} is divided into M time steps, Δt $(\Delta t = t_{max}/M)$. The relationships for the co-ordinate Z_j and the actual solving time t^{i+1} are as follows:

$Zj = \Delta z\,(j-1/2)$, j=1,2,..., N,
$t^{i+1} = t^i + \Delta t$ i=0,1,2,..., M.

The choice of time steps Δt for a non-linear second-order partial differential equation is not straightforward. There are no definite criteria for the choice of Δt due to convergence and stability. This depends on the degree of non-linearity problem, on the employed differences; an implicit scheme: backward or central differences) and matrix stability. In case of the explicit scheme the time step, Δt = 0.05 s was chosen for water and $\Delta t^* = \Delta t/wsp$ for air where wsp > 1. According to the numerical experiment the value wsp = 500 was used. As it appears, the values Δt and wsp are not the optimum. Determination of the optimum values of Δt and wsp was not the aim of this work. The solution was received for the following initial conditions:

$$\theta(z, t=0) = \theta_o$$

$$S_{wo} = \frac{\theta_o}{\varepsilon} = \text{constant.}$$

$$p_a(z, t=0) = p_{atm} \cdot$$

The boundary conditions were as follows:

- for water:

$$q(z=0, t) = 0.736 \cdot K_s ,$$

$$q(z=L, t) = 0 ,$$

- for air:

$$p_a(z=0, t<t_1) = p_{atm} \quad \text{for} \quad S_w < 1 - S_{ra} ,$$

$$q(z=0, t_1 \le t < t_2) = 0 \quad \text{for} \quad p_a \le p_{atm} + p_{ae} ,$$

$$p_a(z=0, t \ge t_2) = p_{atm} \quad \text{for} \; p_a > p_{atm} + p_{ae} ,$$

$$q(z=L, t) = 0 ,$$

where:

t_1 is the time at which the saturation reaches the value equal to S_w=1-S_{ra} at the soil surface, [s],

t_2 is the time at which the soil air pressure p_a equals P_{atm} + p_{ae}, [s],

p_{ae} is the so-called air entry pressure, [dynes/cm^2].

The results shows that also during the initial stage of infiltration when water saturation at the soil surface was small the pore air begins to compress so one can state that P_a>p_{atm}. Initial over pressure of the air is small, though it increases steadily with the amount of water entering the soil. This was supported by all the experimental results (among others, Wilson and Luthin, [1]) and other calculations (among others, Le van Phuc and Morel-Seytoux, [2]).

Results of calculations are shown in figs. 1 and 2. For $p_a(z,t)$ =p_{atm}= constant, the situation exists where there is no entrapped air (air enclosure) and the Richards model can be used (Abo Elela M. I., [10]). This gives different water content distribution profiles $\theta(z, t)$ as they are shown in Fig 2. where results of calculations for double phase **(o)** and single phase (+) models are presented. Also shown in the diagram is another range of wetting front that depends on the selected model on one side (single or double phase) and the initial condition on the other side ($\theta = \theta(z, t=0) = \theta_o$).

The build up model (solved by the computer program CONDUCT written in FORTRAN) allows for a wide range of water infiltration problems into soil profiles.

The boundary conditions for water as well as for air could change with time and could be either Neumann kind or Dirichlet or mixed. For water the upper boundary condition was the Neumann kind. This was automatically verified with respect to water balance in the soil profile, hence the calculations were made for a real q_{real} and not for any potentially possible condition q_{pot} = q where $q = q(z=0, t)$. Among them the following relationship must exist:

$$q_{real}(t) \le q_{pot}(t)$$

In case of one phase model ($p_a(z, t) = p_{atm}$ = constant), the total water infiltration is:

$$\sum q_{real}(t) \cdot \Delta t = \sum q_{pot}(t) \cdot \Delta t ,$$

however for double phase model:

$$\sum q_{real}(t) \cdot \Delta t \le \sum q_{pot}(t) \cdot \Delta t .$$

The analysis of the results shows that, for a high initial water content, even small intensity of infiltration could lead to a substantial increase in pore air pressure which in effect may lead to structural changes in the topmost layer of the soil profile. These structural changes cannot be deduced from the above model, so physical experiments are needed. It is expected that the presented experiments will be helpful in this respect.

The presented results show that the infiltration ability of the soil, for restricted contact of pore air with the atmosphere, is also reduced. It hastens the rise in soil water saturation just below the soil surface.

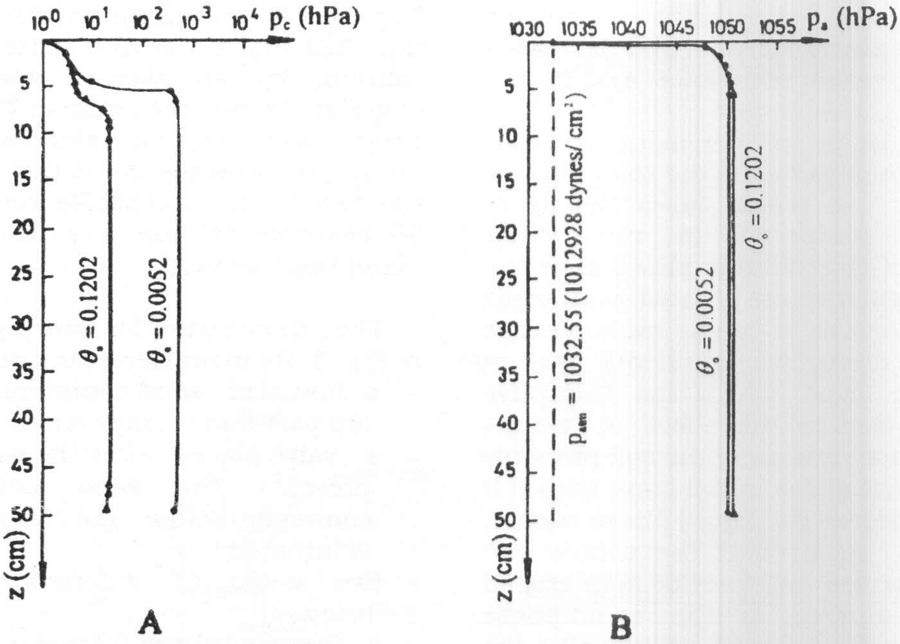

Fig. 1. Calculated values of P_c (A) and P_a (B) at t = 170 s for two cases of initial water content in sand: θ_o = 0.0052 cm³/ cm³ and θ_o = 0.1202 cm³/ cm³.

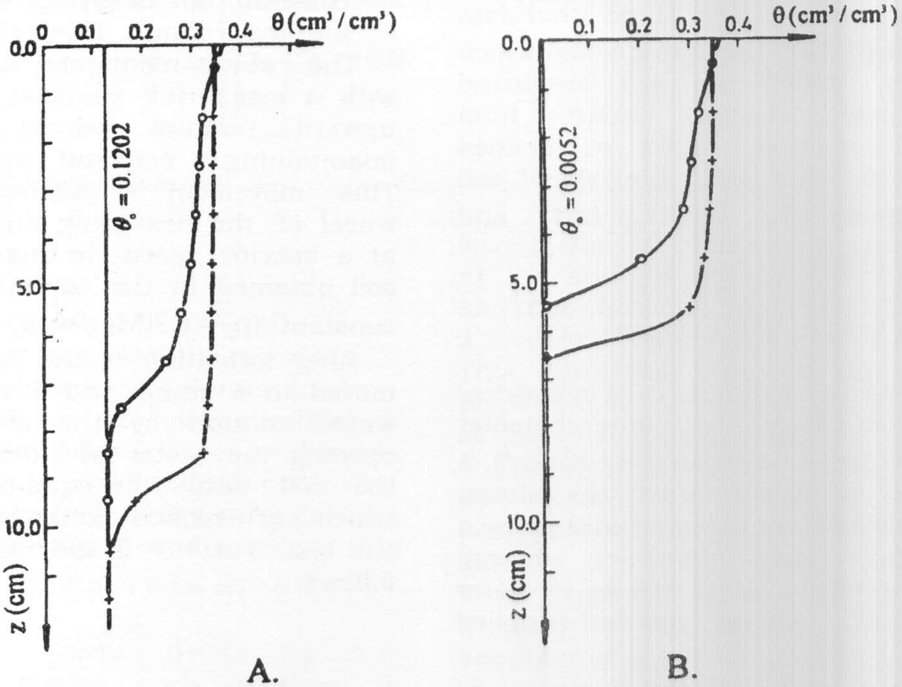

Fig. 2. Calculated soil moisture profiles at t = 170 s for an initial water content θ_o= 0.1202 cm³ cm³ (A) and θ_o = 0.0052 cm³/ cm³ (B): + - infiltration process by Richards equation (p_a = P_{atm}= constant), o – infiltration process by double phase model ($P_a \neq p_{atm}$).

As a result the possibility of pore air contact with the atmosphere further decreases due to the increased resistance against air movement.

This further leads to increasing of the air pressure and then reducing the soil ability to transport water. In some cases the water ability to flow could fall to zero. Other consequences of more vital implication on the safety of soil structure are structural changes in the form of crevices or canals leading to the occurrence of disruptive gradients (as in piping). In the case where the disruptive gradient forms due to the effect of gaseous phase, the internal erosion of the soil probably has a lesser effect at the initial stage than if it is due to the effect of the liquid phase (water). This does not mean that the canals and crevices, etc. formed will not be later eroded (carried to the surface) by the liquid phase when the water finally fills all the underground air pores of the soil, after the escape of the pore air to the atmosphere.

Apart from the changes in water content $\theta(z, t)$, pore air pressure fluctuation $p_a(z, t)$ and capillary pressure $p_c(z, t)$, no other data could be obtained from the above model which could directly define the soil structural changes. These changes apart from experimental detection could be defined through complex theoretical analysis of soil mechanics using the $\theta(z,t), p_a(z,t)$ and $p_c(z, t)$ values obtained.

3. Infiltration test in soil column

The test was carried out in a cylindrical column made of perspex with inner diameter d = 11.28 cm (cross section $S = 100\ cm^2$). A water chamber is placed under the column (Fig. 3). separated from the sand column by a porous ceramic plate (filter) of 10 mm thickness. The sand column was fed by water at its bottom by capillary rise and supplied from the water column (which connected with the ball valve at the bottom of the sand column, by an elastic pipe) to the water chamber below the column. The total column height was 75 cm and the active height (measured from the top of the ceramic filter, to the top of the soil profile in the column) was 50 cm. The column was filled with sand by "sand rain" method.

The device used for pouring sand is shown in Fig. 3. Its main elements are:

- a funneled sand container (bucket) in the top part and it may contain 8.5 kg of sand,
- a valve placed below the sand container. It prevents the sand pouring out the container before the "sand rain" operation is initiated,
- two sieves of different meshes placed below,
- a Perspex tube of 50 mm diameter and 805 mm length. It helps to receive uniform distribution of the falling sand on the surface of the column formed, an indicator (made from brass wire) used to maintain a constant fall height of the sand particles into the column. This height is 65.5 cm.

The above mentioned device is equipped with a measuring pin that helps to keep an upward uniform velocity of the device (maintaining a constant sand falling height). This movement is obtained by rotating the wheel of the measuring pin transmission gear at a specific speed. In this way the density of soil obtained in the column in each test was constant $(\rho_s = 1.7\ Mg/m^3)$.

After formation of the sand column, it is moved to a stand and later connected to the water column by the elastic pipe. After opening the water valve the water enters into the soil until the equilibrium is reached, which corresponds to the initial condition for the test. For t = 0 the initial condition is as follows:

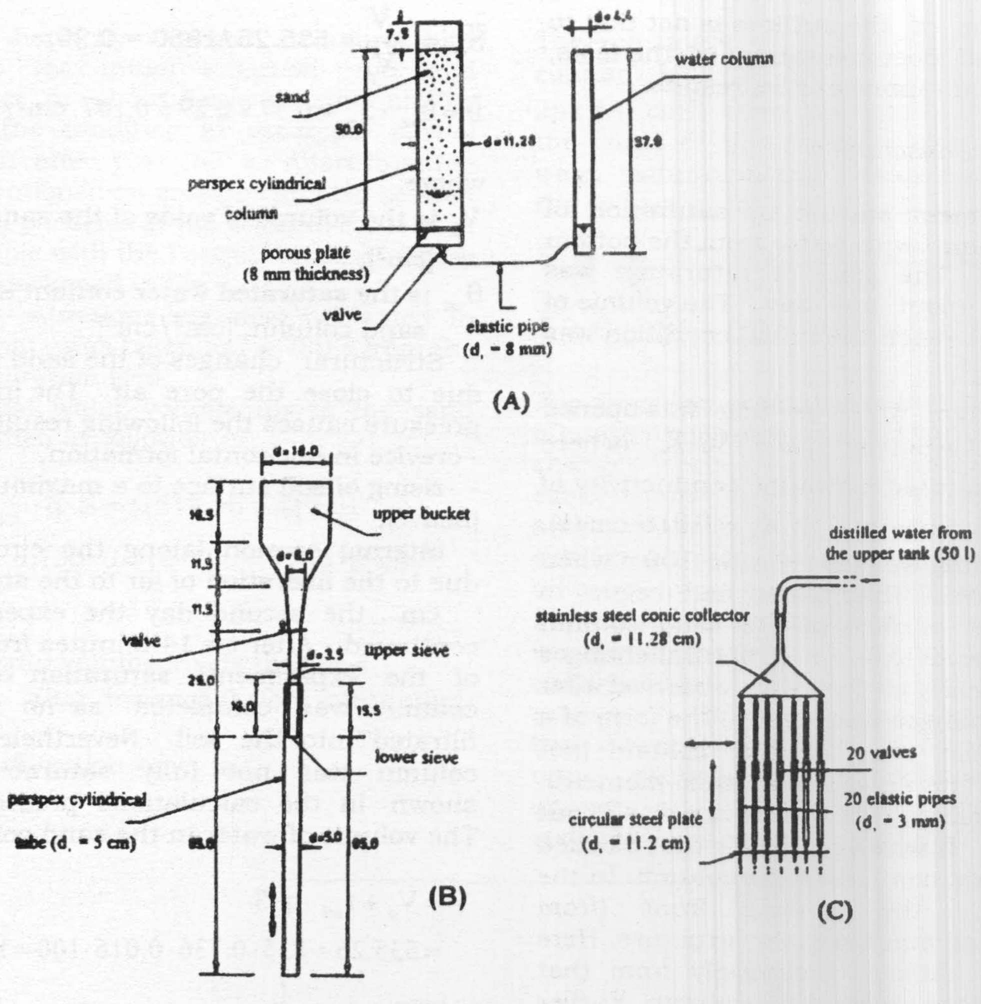

Fig. 3. Physical model (A), sand column filling device (B) and infiltration feeding device (C).

$$h(z, t = 0) = -z,$$

where:

h is the soil water pressure head, [cm],

z is the vertical distance from the top of the filter (bottom of the sand column), [cm].

This equilibrium of the initial condition is obtained after about 7 days. Water level inside the water column is continuously controlled (maintaining water level in the water column at $z = 0$). The measured conductivity of this sand (for $\rho_s = 1.7\ Mg / m^3$) was. $K_s = 1.6 \times 10^{-2}$ cm/s.

The infiltration feeding device, Fig. 3-c, consists of 20 nozzles each of them is connected by an elastic pipe to a valve (similar to ones used in medical drips). All the elastic pipes are joined to top part of the water-feeding device that is in the form of the cone. At the apex of the cone there is a brass tube and cut-off valve. This tube is connected with a tank (of 50 litter capacity) by an elastic pipe. This tank that contains the distilled water helps to maintain a constant outflow condition of water (Mariotte system).

During infiltration, the water-feeding device was released downwards so that the bottom part of each nozzle was about 1 cm above the surface of the sand inside the column. In this way, eventual erosion of the sand surface through the drop of water was prevented. The adoption of nozzle distance (< 1 cm) could lead to upsetting the free formation of the sand surface, caused by several processes taking place inside the soil, e.g. heaving.

The intention of the authors is not that to present the full documentation of the tests, but only selected representative results.

3. 1. Experiment description

This experiment started by saturation of the sand column with water from the bottom (capillary rise). The state of saturation was reached after about one day. The volume of water used to reach the initial condition was $V_o = 417.5\ cm^3$.

The infiltration water feeding was opened with constant intensity $q = 0.736 \cdot K_s$ (where K_s is the saturated hydraulic conductivity of the test sand and equal to $K_s = 0.016$ cm/s). The water feeding was closed after 100 s when it was observed that water had begun to collect on the surface of the sand column (pond). The sand column structural changes started quite early as they were observed after 45 s. These changes were first in the form of a crevice, on the rear of the column (not recorded by the camera at this moment). Maximum thickness of the crevice was about 6 millimeters. It was filled by air that blocked out water movement down the column. In the frontal part, the wetting front (from infiltration) had much regular structure. Here the situation differs completely from that which took place behind the column. Earlier the air released to the atmosphere reduced the size of the sand crevice from 6 mm to 2 mm. At this moment the volume of water inside the column can be expressed as follows:

$$V = V_o + t_{inf} \cdot q \cdot S = 417.5 + 100 \cdot 0.736 \cdot 0.016 \cdot 100$$
$$= 417.5 + 117.5 = 535.26\,cm^3,$$

where:

t_{inf} is the time of infiltration feeding, [s],

q is the infiltration intensity (= $0.736 \cdot K_s$), [cm/s],

S is the cross section area of the column, [cm^2].

Average soil water saturation and average soil water content are:

$$\overline{S}_w = \frac{V}{V_p} = 535.26/1850 = 0.29,$$

$$\overline{\theta} = \theta_{sat} \cdot \overline{S}_w = 0.37 \times 0.29 = 0.107\ cm^3/cm^3,$$

where:

V_p is the volume of voids of the sand column, [cm^3],

θ_{sat} is the saturated water content inside the sand column, [cm^3/cm^3].

Structural changes of the sand column are due to close the pore air. The increased air pressure causes the following results:

- crevice in horizontal formation,
- rising of soil surface to a maximum of 5 mm (heave),
- internal erosion (along the circumference) due to the liberation of air to the atmosphere.

On the second day the experiment was continued. After t = 14 minutes from the start of the experiment) saturation of the sand column was completed as no more water filtrated into the soil. Nevertheless the sand column was not fully saturated which is shown in the calculations presented below. The volume of water in the sand column is:

$$V = V_o + t_{inf} \cdot q \cdot S.$$
$$= 535.26 + 835 \cdot 0.736 \cdot 0.016 \cdot 100 = 1518.56\,cm^3.$$

Therefore the average water saturation and the average water content in the soil are as follows:

$$\overline{S}_w = \frac{V}{V_p} = 1518.56/1850 = 0.821 < 1.0,$$

$$\overline{\theta} = \theta_{sat} \cdot \overline{S}_w = 0.37 \cdot 0.821 = 0.304\ cm^3/cm^3 < 0.37\ cm^3/cm^3.$$

From the above one can see that the volume of sand column pores filled by air is $331.4\ cm^3$, i.e. 17.9 % $= (1.0 - S_w) \times 100\,\%$.

In the next stage the sand column was affected by drainage. The infiltration water feed again started. After t = 150 s, a clear crack (fissure) was observed in the sand column and it was arranged in almost horizontal formation dividing the sand column into two different parts: the bottom part with undisturbed structure and the top smaller part with distinctly changed structure. With respect to the initial situation the sand surface rose to about 8 mm (maximum). Fig. 4, shows the condition at the upper part of the column after t = 150 s. Apart from the cracks mentioned an erosion can also be seen (absence of particles at the internal contact, of sand sample with the Perspex surface). These places are darkened in Fig 4.

Similar situations are also presented in Photo 1 that was taken at t = 780 s from the start of infiltration feed.

The total water volume inside the sand column is then as follows:

$$V = V_o + t_{inf} \cdot q \cdot S = (1518.56 - 417.0) + 140 \cdot 0.736 \cdot 0.016 \cdot 100 = 1266.42\,cm^3,$$

where:

V_o is the water volume inside the sand column after drainage (before infiltration), [cm^3],

t_{inf} is the infiltration time, [s].

The remaining volume of water in the sand column is less (by 1518.56 − 1266.42 = 252.14 cm^3) than the volume of water before the start of the drainage test. The average water saturation and average water content of the soil are as follows:

$$\overline{S}_w = \frac{V}{V_p} = 1266.42/1850 = 0.685$$

$$\overline{\theta} = \theta_{sat} \cdot \overline{S}_w = 0.37 \cdot 0.685 = 0.253\ cm^3/cm^3.$$

The described experiments that were tested for 50 days clearly documented various structural changes during water infiltration into a dry sand sample as well as into a sand sample after drainage of the earlier completely saturated soil. These changes may have different forms as for example ducts (arranged vertically) or fissures entering deeply into the sample (in horizontal arrangement). The last changes could affect on the whole cross section of the sand column that could lead to the separation of the column sample into the upper section with pronounced structural changes and bottom section with unnoticed structural changes

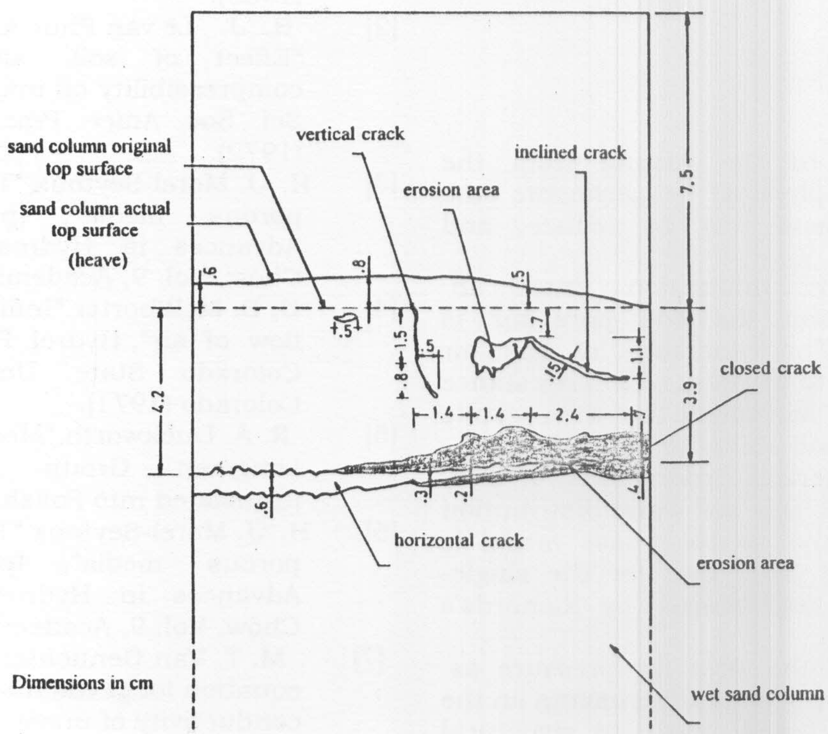

Fig. 4. Positions and dimensions of cracks in the rear part of the sand column at t = 150 s (counted from the third start of water feeding as feeding time equal to 140 s).

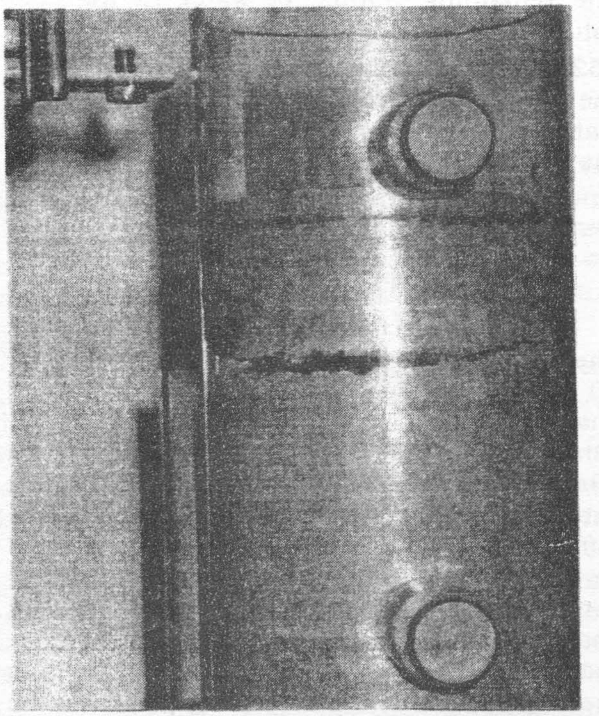

Photo 1. Situation on the upper side of the sand column after t=780 s (counted from the third start of water feeding as feeding time equal to 140 s), the clear fissure and heave can be seen.

4. Conclusions

With regard to the results from the numerical and physical experiments the following conclusions can be deduced and formulated:

1. During water infiltration into an unsaturated soil the soil pore air is compressed. The increase of the air pressure leads to increase of soil resistance against water movement that then results to a fall in the soil ability to infiltration.
2. From the numerical experiments, it was discovered that the soil water distribution obtained for the double phase model is quite different from that for the single-phase model represented by Richards's equation.
3. Generation of the pore air pressure as shown by the physical experiments on the sand column could lead to structural changes in the soil particularly in the upper part below the surface. The structural changes could take the form of crevices or blisters filled with air, surface heave, formation of canals (piping), etc. During infiltration, the air bubbles on the topsoil surface may be formed. Generation of the soil air pressure by infiltration of water, into an unsaturated soil structure could lead to unfavorable soil structural changes which as a result could impend over safety or stability failure of, e.g. foundation, slope, etc.
4. In the case of water infiltration into an unsaturated soil profile the phenomenon of an unstable wetting front could lead to the trapping of soil air. The entrapped soil air pressure, p_a, could be much greater than the atmospheric pressure ($p_a \geq p_{atm}$) and that of the surrounding.

References

[1] L. G. Wilson J. N. and Luthin, "Effect of air-flow ahead of the wetting front on infiltration", Soil Sci., 96, pp. 136-143 (1963).

[2] H. J. Le van Phuc and Morel-Seytoux, "Effect of soil air movement and compressibility on infiltration rates", Soil Sci. Soc. Amer. Proc., 36, pp. 237-241 (1972).

[3] H. J. Morel-Seytoux "Two-phase flows in porous media", (pp. 119-202) in: Advances in Hydroscience, ed. vente Chow, Vol. 9, Academic Press (1973).

[4] D. B. McWhorter "Infiltration affected by flow of air", Hydrol. Pap., Vol. 49, p. 43, Colorado State Univ., Fort Collins, Colorado (1971).

[5] R. A. Duckworth "Mechanics of Fluids", Longman Group Limited, London (translated into Polish, 1983) (1977).

[6] H. J. Morel-Seytoux "Two-phase flows in porous media", (pp. 119-202) in: Advances in Hydroscience, ed. vente Chow, Vol. 9, Academic Press (1973).

[7] M. T. Van Genuchten "A closes form equation for predicting the hydraulic conductivity of unsaturated soils", Soil

Sci. Soc. Amer. J., 44, pp. 892-898 (1980).

[8] R. H. Brooks A. T. and Corey, "Properties of porous media affecting fluid flow", J. Irrig. Drain. Div. Amer. Soc. Civ. Eng., 92 (2), pp. 61-68 (1966).

[9] H. Zaradny H., "Groundwater Flow in Saturated and Unsaturated Soil"A. A. Balkema/Rotterdam/Brookfield (1993).

[10] M. I. Abo Elela "Numerical model for one dimensional vertical water flow in soil profile", Proceed. Intern. AMSE Conf. "Information Methods for engineering Problems", Malta, Dec. 28-30, AMSE Press, 2, pp.151-162 (1993).

Received November 14, 1999
Accepted January 6, 2000